Plant, Cell & Environment

Plant, Cell and Environment (2014) **37**, 1022–1036 doi: 10.1111/pce.12218

Original Article

The purine metabolite allantoin enhances abiotic stress tolerance through synergistic activation of abscisic acid metabolism

Shunsuke Watanabe[1], Mayumi Matsumoto[2]*, Yuki Hakomori[2]*, Hiroshi Takagi[1], Hiroshi Shimada[1,2] & Atsushi Sakamoto[1,2]

[1]*Department of Mathematical and Life Sciences, Graduate School of Science and* [2]*Department of Biological Science, Faculty of Science, Hiroshima University, 1-3-1 Kagamiyama, Higashi-Hiroshima 739-8526, Japan*

ABSTRACT

Purine catabolism is regarded as a housekeeping function that remobilizes nitrogen for plant growth and development. However, emerging evidence suggests that certain purine metabolites might contribute to stress protection of plants. Here, we show that in Arabidopsis, the intermediary metabolite allantoin plays a role in abiotic stress tolerance via activation of abscisic acid (ABA) metabolism. The *aln* loss-of-function of *ALN*, encoding allantoinase, results in increased allantoin accumulation, genome-wide up-regulation of stress-related genes and enhanced tolerance to drought-shock and osmotic stress in *aln* mutant seedlings. This phenotype is not caused by a general response to purine catabolism inhibition, but rather results from a specific effect of allantoin. Allantoin activates ABA production both through increased transcription of *NCED3*, encoding a key enzyme in ABA biosynthesis, and through post-translational activation via high-molecular-weight complex formation of BG1, a β-glucosidase hydrolysing glucose-conjugated ABA. Exogenous application of allantoin to wild-type plants also activates the two ABA-producing pathways that lead to ABA accumulation and stress-responsive gene expression, but this effect is abrogated in ABA-deficient and *BG1*-knockout mutants. We propose that purine catabolism functions not only in nitrogen metabolism, but also in stress tolerance by influencing ABA production, which is mediated by the possible regulatory action of allantoin.

Key-words: *Arabidopsis thaliana*; ABA-GE; BG1; NCED3; metabolic intermediate; purine catabolism; stress response; ureide.

INTRODUCTION

Purine compounds have vital roles in many biological processes as key components of heredity, signalling, bioenergetics and cellular metabolism. Moreover, certain bacteria and fungi can use purine bases as a nitrogen source, a widespread strategy for survival under nutrient-deficient conditions (Vogels & Van der Drift 1976). Plants are also able to mineralize purines to inorganic nitrogen, an essential but environmentally scarce macronutrient that is required for proper growth and development (Stasolla *et al*. 2003). Therefore, it has generally been accepted, though not yet demonstrated experimentally, that the main function of purine catabolism in plants is to recycle nitrogen for remobilization to support new growth and reproduction (Zrenner *et al*. 2006).

Plant purine catabolism has a relatively long history of physiological and biochemical studies, particularly in leguminous species because it constitutes an integral part of the storage and xylem translocation of symbiotically fixed nitrogen (Schubert 1986; Smith & Atkins 2002). Only recently, however, have the pathway and the enzymes involved in each step of purine catabolism been identified at the molecular and biochemical levels, mainly using the model plant *Arabidopsis thaliana* (Werner & Witte 2011). Xanthine is the first common intermediate of the degradation of all purine bases that originate from AMP (Fig. 1a; Stasolla *et al*. 2003; Zrenner *et al*. 2006). Therefore, xanthine oxidation is a critical step in the purine-catabolic pathway, which is distributed across the cytosol, peroxisome and endoplasmic reticulum (ER). This linear pathway involves seven enzymes that allow conversion of xanthine, through urate, to allantoin, followed by its sequential hydrolysis to release four ammonium ions.

Although attributed to source-to-sink nitrogen remobilization, the role of purine degradation might not be restricted to housekeeping tasks, as several recent reports cite its close association with plant responses and adaptation to stress. For example, various plants respond to abiotic and biotic stress by inducing and activating enzymes in the purine degradation pathway (Montalbini 1995; Sagi *et al*. 1998; Hesberg *et al*. 2004; Yesbergenova *et al*. 2005; Alamillo *et al*. 2010). This activation often results in increased levels of intermediary metabolites, particularly allantoin and allantoate, under stress conditions (Montalbini 1991; Sagi *et al*. 1998; Nikiforova *et al*. 2005; Brychkova *et al*. 2008; Alamillo *et al*. 2010; Kanani *et al*. 2010; Rose *et al*. 2012; Yobi *et al*. 2013). More recently, reverse genetic approaches have been adopted to examine the role of purine catabolism in plant physiological processes including growth, development and stress responses. For example,

Correspondence: A. Sakamoto, Fax: +81 (0)82 424 4530; e-mail: ahkkao@hiroshima-u.ac.jp

*M.M and Y.H. equally contributed to this work.

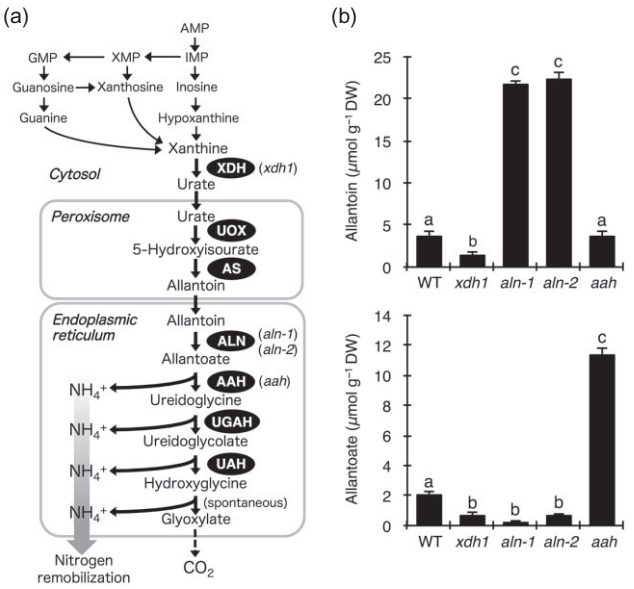

Figure 1. Plant purine catabolism and knockout mutants used in this study. (a) The catabolic pathway. Only enzymes involved in the main catabolic pathway starting from xanthine are shown and knockout mutants used in this study are indicated in parentheses after abbreviated enzyme names. AAH, allantoate amidohydrolase; ALN, allantoinase (allantoin amidohydrolase); AS, allantoin synthase; UAH, ureidoglycolate amidohydrolase; UGAH, ureidoglycine aminohydrolase; UOX, urate oxidase; XDH, xanthine dehydrogenase. Note that, besides xanthine oxidation, XDH also catalyses the conversion of hypoxanthine to xanthine. (b) Levels of two major ureides, allantoin and allantoate, in aseptically grown 2-week-old seedlings of four knockout mutants of purine degradation used in this study (Supporting Information Figs S1–S3). DW, dry weight. Results are the mean of five independent experiments ± standard errors of means. Different letters indicate significant difference among genotypes by one-way analysis of variance with Tukey's multiple comparison test ($P < 0.05$).

Arabidopsis mutants defective in xanthine dehydrogenase (XDH), the critical bottleneck to purine oxidation and subsequent ureide hydrolysis (Fig. 1a), display precocious senescence (Nakagawa *et al*. 2007a; Brychkova *et al*. 2008) and become hypersensitive to drought stress (Watanabe *et al*. 2010) and prolonged dark incubation (Brychkova *et al*. 2008). The *xdh* mutant phenotypes are restored to normal by administration of a downstream metabolite (urate, allantoin or allantoate), suggesting the existence of mechanisms involving purine catabolites to modulate physiological processes and stress adaptation (Nakagawa *et al*. 2007a; Brychkova *et al*. 2008; Watanabe *et al*. 2010).

Despite the possible role of purine catabolites in plant responses and adaptation to abiotic stress, it remains unclear how these compounds contribute to stress protection, as attempts to define the precise role(s) have so far been limited to exogenous administration experiments. Such studies using root tips or leaf discs have suggested that allantoin and allantoate, the major purine metabolites in stressed plants including Arabidopsis, protect plants from oxidative damage by scavenging reactive oxygen species (Gus'kov *et al*. 2004; Brychkova *et al*. 2008). However, the amounts of these ureides are relatively low, even under stress conditions (e.g. below 1 μmol g^{-1} fresh weight in Arabidopsis; Brychkova *et al*. 2008), compared with major antioxidants such as ascorbic acid. Moreover, *in vitro* assessment of antioxidant capacity argues against such a possibility (Wang *et al*. 2012). Therefore, there is a clear need to investigate the possible mechanisms of action of these metabolites in plant acclimatization to abiotic stress.

In this study, we examined the consequences of constitutively elevated levels of allantoin caused by Arabidopsis knockout mutants of allantoin amidohydrolase (allantoinase: ALN), together with the other two knockout mutants of XDH and allantoate amidohydrolase (AAH) that are defective in different steps in the purine-catabolic pathway (Fig. 1a). We reasoned that if allantoin is intrinsically important in protecting plants against stress, its constitutive accumulation might improve plant performance under stress, thereby providing clues to the *in planta* mechanism by which this purine metabolite acts in stress protection. We show that the *ALN*-knockout (*aln*) mutation, but not the other two mutations in the degradation pathway, enhanced drought and osmotic tolerance in Arabidopsis. The phenotype of the *aln* mutants seemed to result from up-regulation of stress-responsive genes through activation of the biochemical pathways leading to abscisic acid (ABA) accumulation, which also could be induced in wild-type (WT) plants by administering exogenous allantoin. However, the effect of exogenous allantoin was totally blocked by mutations impairing ABA production. Our results thus indicate that purine catabolism is involved in the defence against abiotic stress in Arabidopsis, including through a previously unknown regulatory effects of allantoin, as elevated allantoin levels synergistically activate ABA metabolism and elicit ABA-mediated stress responses.

MATERIALS AND METHODS

Plant materials and growth conditions

Arabidopsis [*A. thaliana* (L.) Heynh.] accession Columbia-0 (Col-0) was used as WT and all mutant lines used in this work were in the Col-0 background. The seeds of *aba2-1* mutant (CS156; Léon-Kloosterziel *et al*. 1996) and the following SALK T-DNA insertion lines were obtained from the Arabidopsis Biological Resource Center (Ohio State University): *aln* (SALK_000325; Yang & Han 2004; also called *aln-1* in this work) and *aln-2* (SALK_146783, this study) disrupted in *ALN* (At4g04955); *xdh1* (SALK_148366, this study; with the identical insertion site to SALK_148368 described in Yesbergenova *et al*. 2005) disrupted in *XDH1* (At4g34890); *aah* (SALK_112631; Todd & Polacco 2006) disrupted in *AAH* (At4g20070); and *bglu18* (SALK_075731C; Ogasawara *et al*. 2009) disrupted in *BGLU18* (At1g52400; also known as *BG1*). To identify homozygous T-DNA insertion lines, PCR-based genotyping of each mutant was performed using a gene-specific primer flanking the insertion in combination with a left-border T-DNA-specific LBa1 primer (Supporting

Information Table S1). Surface-sterilized seeds from WT and transgenic plants were sown on 0.3% (w/v) gellan gum plates of standard medium consisting of half-strength Murashige-Skoog (1/2MS) basal salts and 1% (w/v) sucrose. After incubation at 4 °C, for 2 d, the plates were placed in a growth cabinet maintained at 22 °C under white fluorescent light with a 16-h photoperiod (70 μmol photons m^{-2} s^{-1}).

Genetic complementation

The complete *ALN* coding sequence was generated by PCR from cDNA made from total RNA of WT seedlings (for primers, see Supporting Information Table S1). After sequence verification, the *ALN* coding sequence was cloned into pGWB14 (Nakagawa *et al*. 2007b) under the control of the cauliflower mosaic virus (CaMV) 35S promoter. The resulting recombinant binary plasmid carried by *Agrobacterium tumefaciens* strain GV3101 was introduced into the homozygous *aln-1* mutant plants through the floral-dip method as previously described (Clough & Bent 1998).

Stress treatments and assays

Drought shock was imposed as described in Watanabe *et al*. (2010). Aseptically grown 2-week-old seedlings were carefully removed from gellan gum plates and exposed to the air on a dry filter paper for 60 min. Alternatively, moist filter papers were used instead as control treatments. Wilted plants were then transferred back to gellan gum plates and allowed to recover for 7 d under the growth condition as described above. Survival was evaluated by counting seedlings showing total chlorosis as dead. To test osmotic stress tolerance, plants were grown on gellan gum plates of standard medium supplemented with mannitol, or on agar plates [1.5% (w/v) agar] that were infused with polyethylene glycol (PEG 8000; Sigma-Aldrich, St Louis, MO, USA) to give a water potential of approximately –0.5 MPa according to the published protocol (Verslues *et al*. 2006). Sterilized seeds were sown on these media, and after a 2 d cold treatment, seedlings were grown in a growth chamber as described above. Alternatively, normally grown 3-day-old sterile seedlings were transplanted onto mannitol medium. Dry or fresh weight was scored after 14 d of growth or transplanting. Relative growth is expressed as a percentage of a whole plant weight in the absence of stress.

Determination of allantoin, allantoate and chlorophyll

Allantoin and allantoate were determined after chemical transformation to glyoxylate by heat-induced alkaline-acid hydrolysis and acid hydrolysis, respectively (Todd & Polacco 2006). Chlorophyll was quantified as described previously (Nakagawa *et al*. 2007a).

qRT-PCR

Total RNA was prepared from aerial parts of aseptically grown 2-week-old plants using the NucleoSpin RNAII extraction kit (Macherey-Nagel GmbH & Co, Düren, Germany). First-strand cDNA was synthesized using 1 μg total RNA as a template, an oligo(dT) 18-mer primer and the ReverTra Ace qPCR RT kit (Toyobo, Osaka, Japan). Levels of various mRNAs were quantified by qRT-PCR using the KAPA SYBR FAST qPCR Kit (Kapa Biosystems, Inc., Woburn, MA, USA) in a 7300 Real-Time PCR System (Applied Biosystems, Foster City, CA, USA). All PCR amplifications contained 1 × KAPA SYBR Green Master Mix, 0.2 μM each primer and 10 ng cDNA (total RNA equivalent) in a total volume of 20 μL. Gene-specific PCR primers were designed using Primer3Plus (http://www.bioinformatics.nl/cgi-bin/primer3plus/primer3plus.cgi) and primer sequences are listed in Supporting Information Table S1. Relative gene expression data were analysed using the comparative $2^{-\Delta\Delta Ct}$ method (Livak & Schmittgen 2001) after normalization with *ACT2* as the control transcript.

Microarray analysis

Total RNA was extracted from 2-week-old WT and *aln-1* seedlings as described above. Two independent biological samples were used per genotype. Target labelling and hybridization to Affymetrix ATH1 GeneChips were performed according to the manufacturer's instructions at the Analysis Center of Life Science, Hiroshima University. Hybridization signals were acquired using an Affymetrix GeneChip Scanner 3000 7G; raw array images were analysed using the MAS5 algorithm in GeneSpring GX software version 12 (Agilent Technology, Palo Alto, CA, USA) to normalize probe sets. At the gene enumeration steps, control probe sets, ambiguous probe sets that were mapped to no or multiple loci in the TAIR10 genome annotation (http://www.arabidopsis.org), and probes for organelle-encoding genes were removed, while redundant probe sets representing the same locus were counted only once. Genes of interest were classified into functional categories using the Munich Information Center for Protein Sequences (MIPS) Functional Catalog *Arabidopsis* Database (Ruepp *et al*. 2004; http://mips.helmholtz-muenchen.de/proj/funcatDB/). The data reported in this paper have been deposited in the Gene Expression Omnibus (GEO) database, http://www.ncbi.nlm.nih.gov/geo (accession no. GSE44922).

Promoter reporter assay

A 5′-upstream region (–1356 to + 125 bp relative to the transcription start site) of the gene encoding Arabidopsis 9-*cis*-epoxycarotenoid dioxygenase 3 (NCED3) was obtained by PCR (for primers, see Supporting Information Table 1), sequenced and cloned into pUGW35 (Nakagawa *et al*. 2007b) to direct transcription of a firefly luciferase (Fluc) reporter gene. This plasmid was introduced into rosette leaves of 2-week-old seedlings by particle bombardment (PDU-1000/He, Bio-Rad, Hercules, CA, USA), together with an internal control plasmid carrying a *Renilla reniformis* luciferase (Rluc) gene driven by the CaMV 35S promoter. After bombardment, the plants were kept in the dark for 18 h

Table 1. Top 10 most significantly overrepresented functional subcategories in the *aln-1* mutant

FunCat number[a]	Functional subcategory	Observed frequency (%)	Expected frequency (%)	*P*-value
32.01.03	Osmotic and salt stress response	5.00	0.72	1.60×10^{-10}
34.11.03.13	Osmosensing and response	5.00	0.73	2.03×10^{-10}
36.20.18.05	Abscisic acid response	4.16	0.56	2.42×10^{-10}
32.01	Stress response	9.44	2.92	2.49×10^{-10}
01.20	Secondary metabolism	6.11	1.49	3.34×10^{-8}
34.11.03	Chemoperception and response	8.88	2.95	3.98×10^{-8}
34.11.03.12	Water response	3.05	0.41	3.61×10^{-7}
34.11	Cellular sensing and response to external stimulus	11.9	5.24	4.51×10^{-7}
36.20.18	Plant hormonal regulation	6.11	2.07	7.48×10^{-6}
20.01	Transported compounds (substrates)	13.0	6.65	7.96×10^{-6}

The functional classification was performed for 361 genes that were at least 3.0-fold up-regulated in the *aln-1* mutant using the MIPS interface (http://mips.helmholtz-muenchen.de/proj/funcatDB/), and functional subcategories (after the second hierarchical level) were ranked by their *P*-values, which were determined by comparing the observed with the expected frequencies for each functional subcategories using the hypergeometric distribution method.

[a]Functional catalogue number assigned to each of MIPS functional subcategories.

before enzyme assay. Fluc and Rluc activities were measured using the Dual Luciferase Reporter Assay system (Promega, Madison, WI, USA) following the manufacturer's instructions. Chemiluminescence was recorded on a microplate chemiluminometer (LB941; Berthold Technologies, Bad Wildbad, Germany). The data obtained were expressed as Fluc activity normalized to Rluc activity.

Measurement of stomatal apertures

Stomatal aperture was measured by microscopy of a leaf epidermal strip. To prepare epidermal samples, the adaxial side of each leaf was stuck to transparent adhesive tape, and the epidermal layer was peeled from the abaxial side with another strip of adhesive tape. The resulting epidermal strips were examined for stomatal size by optical microscopy (Eclipse 80i; Nikon, Tokyo, Japan). Stomatal responses to ABA were examined according to Pei *et al*. (1997) with slight modification. Detached leaves were floated on 10 mM 2-(*N*-morpholino)-ethanesulfonic acid buffer (pH 6.5) containing 50 mM KCl and 0.1 mM $CaCl_2$ for 2 h under continuous light to ensure that stomata were open. After an additional incubation for 3 h in the presence or absence of ABA, widths of stomatal apertures were determined as described above.

Determination of ABA, its hydrolysable conjugates and hydrolysis activity

The levels of free and conjugated forms of ABA were measured using an enzyme-linked immunosorbent assay (ELISA) as described previously (Dietz *et al*. 2000; Yan *et al*. 2007). Aerial parts of 2-week-old plants were ground in liquid nitrogen to a fine powder. Ground tissues were suspended in 80% (v/v) methanol containing 0.5 g L^{-1} citric acid monohydrate and 100 mg L^{-1} dibutylhydroxytoluene, and stirred overnight in the dark at 4 °C. The suspension was cleared by centrifugation at 1000 *g* for 20 min, and the supernatant was dried under vacuum. The resulting solid residue was dissolved in absolute methanol and added to Tris-buffered saline (TBS: 50 mM Tris-HCl, pH 7.8, 0.1 mM $MgCl_2$ and 0.15 M NaCl) in a 1:9 volume ratio to measure free ABA. For preparation of the hydrolysable conjugate ABA-*β*-D-glucosyl ester (ABA-GE), the powdered tissues were lysed with 10 mM $CaCl_2$ for 24 h at 4 °C and centrifuged at 20 000 *g* for 10 min. The supernatant was acidified to pH 3.0 with 0.1 M HCl and then extracted thrice with ethyl acetate to remove free ABA. The aqueous fractions containing ABA conjugates were hydrolysed with 1 M NaOH, after which the released ABA was acidified, partitioned into ethyl acetate and dried as described above. ELISA-based quantification was performed using the ABA Immunoassay detection kit (Sigma-Aldrich) according to the provided protocol.

ABA-GE hydrolysis activity was measured in microsomal fractions as described previously (Lee *et al*. 2006). Frozen seedlings were powdered in liquid nitrogen and homogenized with ice-cold lysis buffer (25 mM HEPES, pH 7.0, 250 mM sucrose, 10 mM $MgCl_2$ and 1 mM dithiothreitol). After the homogenate was centrifuged at 10 000 *g* at 4 °C for 5 min, the cleared supernatant was centrifuged at 100 000 *g* at 4 °C for 1 h to precipitate microsomes. The microsomal pellets were resuspended in lysis buffer containing 1% (v/v) Triton X-100, and the aliquots were assayed for enzyme activity that liberates free ABA from its glucose conjugates by incubating with 100 nM ABA-GE (OlChemim Ltd, Olomouc, Czech Republic) at 37 °C for 1 h. After incubation, the liberated ABA was measured using ELISA, as described above.

Fractionation of native proteins by gel filtration column chromatography

Proteins were fractionated according to their native size by gel filtration column chromatography essentially as described previously (Lee *et al*. 2006). Aerial parts of 2-week-old plants were homogenized in 50 mM sodium phosphate buffer (pH 7.0) containing 150 mM NaCl, 0.02% (w/v) NaN_3, 10 mM

dithiothreitol and 0.1% (v/v) Triton X-100, and centrifuged twice at 14 000 *g* at 4 °C for 10 min. After filtration through a membrane filter (DISMIC-13HP-PTFE, 0.45 μm pore size; Advantec, Tokyo, Japan), the supernatant was loaded onto a HiPrep16/60 Sephacryl S-300 high-resolution column using the ÄKTA*explorer* 10S system (GE Healthcare, Uppsala, Sweden). For protein elution, the flow rate was adjusted to 0.5 mL min^{-1} and 3.0 mL fractions of effluent were collected with the above buffer, without Triton X-100. An aliquot of each fraction was separated by sodium dodecyl sulphate-polyacrylamide gel electrophoresis (SDS-PAGE) using a 10% gel and transferred onto a polyvinylidene difluoride membrane (Immobilon-P; Millipore, Billerica, MA, USA). After blocking in 0.3% (w/v) skim milk, the blotted membrane was incubated with primary antibodies. The following antibodies were each used at 1:2000 dilution: anti-BG1/BGLU18 (Ogasawara *et al*. 2009), anti-glutamine synthetase (anti-GS; Sakamoto *et al*. 1990) and anti-nitrite reductase (anti-NiR; Shigeto *et al*. 2006). The membrane was then probed with anti-rabbit IgG secondary antibody conjugated to horseradish peroxidase (at 1:5000 dilution). Antigen-antibody complexes were detected in a chemiluminescence reaction using the Western Lighting Plus-ECL kit (Perkin-Elmer Life Sciences, Wellesley, MA, USA) and digitally captured on the VersaDoc 5000 imaging system using Quantity One software (Bio-Rad Laboratories).

Statistical analysis

All results are presented as means and standard errors of means. The difference between two groups was evaluated using Student's or Welch's *t*-test, depending on whether the variances of the compared samples were regarded as equal or not. Comparisons among three or more groups were made using one-way analysis of variance with Tukey's multiple comparison test, following Bartlett's test for homogeneity of variance. Testing was performed using R statistical software (version 2.15.2, R Development Core Team, Vienna, Austria).

RESULTS

Gene knockout of the enzymes involved in purine catabolism results in differential allantoin accumulation

To investigate the possible effects of constitutive allantoin accumulation on stress tolerance in *Arabidopsis*, we obtained two loss-of-function alleles for *ALN* from the SALK Institute T-DNA insertion collection. One insertion line (SALK_000325) was previously described as *aln* (Yang & Han 2004), and the other (SALK_146783) was newly characterized in this study (Supporting Information Fig. S1). For clarity, here we refer to the previously identified allele as *aln-1* and the newly characterized allele as *aln-2*. The results from PCR genotyping, qRT-PCR, and growth assays supported that each allele causes a defect in allantoin catabolism (Supporting Information Fig. S1). In order to distinguish the specific effects of allantoin accumulation from general inhibitory effects on the purine-catabolic pathway, in this study, we also examined two other catabolic mutants, *xdh1* and *aah* (Supporting Information Figs S2 & S3), which are defective in catabolic steps upstream and downstream of allantoin degradation, respectively (Fig. 1a). Compared with WT, the steady-state allantoin levels increased sixfold in both *aln-1* and *aln-2* mutants; by contrast, *xdh1* mutants exhibited significantly lower allantoin levels and *aah* mutants exhibited allantoin levels comparable to WT (Fig. 1b). Allantoate, the immediate downstream metabolite of allantoin, accumulated about sixfold more in the *aah* mutant but decreased significantly in *xdh1* and *aln* mutants (Fig. 1b). The differential pattern of ureide accumulation signifies the specific step at which the catabolic pathway was impaired in each mutant.

aln mutation enhances drought and osmotic stress tolerance

We tested the tolerance of the *aln* mutants to water-deficit conditions created by drought shock or high osmoticum. Firstly, we exposed 2-week-old sterile WT and *aln* seedlings to 60 min of air-drying, as we have done previously (Watanabe *et al*. 2010). After the treatment, when the wilted plants were returned to standard medium and allowed to grow for 7 d, only 66% of WT plants recovered (Fig. 2a,b). In contrast, more than 85% of both *aln-1* and *aln-2* plants survived to maturity possibly because, upon recovery from drought shock, these *aln* mutants had better growth and more chlorophyll than WT plants (Fig. 2c,d). To ascertain whether a mutation in the *aln* gene was responsible for the observed phenotype, the *aln-1* mutant was transformed with a complementation construct. Restoring *ALN* expression by genetic complementation reversed the drought-tolerant phenotype of the *aln-1* mutant (Fig. 2a,b) as well as the ureide levels (Supporting Information Fig. S4). These results indicate that loss-of-function mutations in the *ALN* gene resulted in enhanced drought-shock tolerance in Arabidopsis.

Next, we tested whether the *aln* mutants enhance the ability to tolerate osmotic stress. In the presence of high osmolarity imposed by mannitol (100, 150 and 200 mM), the rates of seed germination were not significantly different between WT and the two *aln* mutants (Supporting Information Fig. S5). However, after growth for 14 d on mannitol media, the *aln* mutants grew better than WT (Fig. 3a,b), suggesting that they are more tolerant to osmotic stress during seedling development. Corroborating results were obtained when post-germinated seedlings were subjected to 200 mM mannitol and the growth was compared between WT and *aln* mutants (Fig. 3c,d). To further test the generality of osmotic stress responses, we exposed the *aln*, *xdh1* and *aah* mutants to another osmotic stress agent, PEG. As in the case of mannitol, the susceptibility at germination stage did not differ significantly among these genotypes (Supporting Information Fig. S6). However, when grown for 27 d in medium with low water potential imposed by PEG, the two *aln* mutants had significantly more fresh weight as compared with WT or the

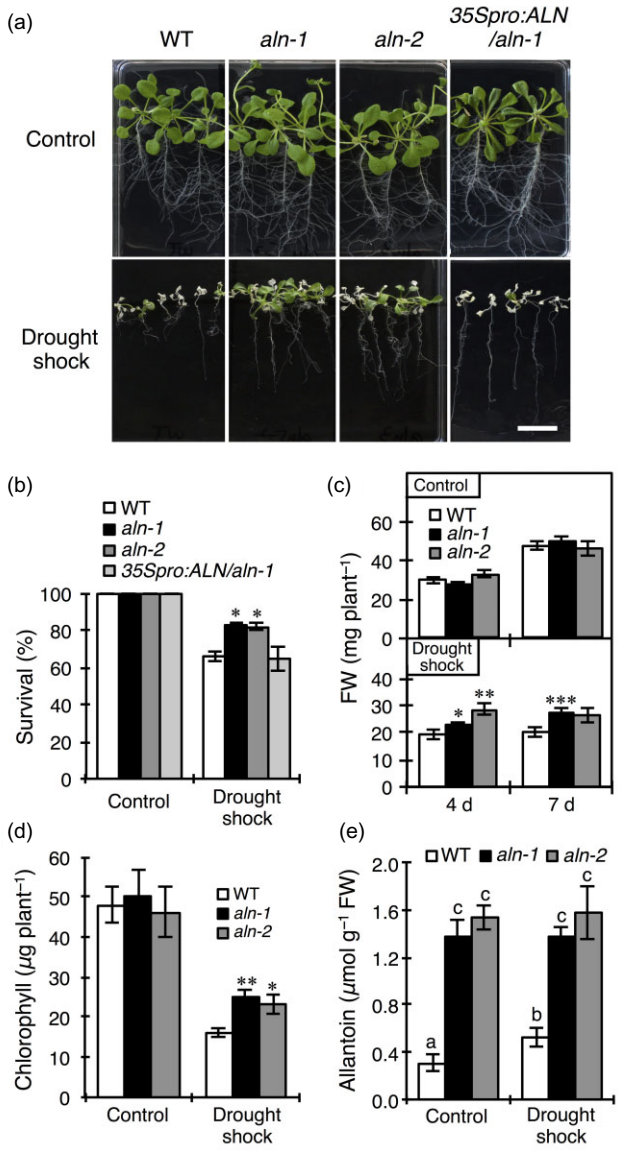

Figure 2. Tolerance of *aln-1* and *aln-2* mutants to drought shock. Aseptically grown 2-week-old seedlings from wild type (WT), two *aln* mutants and *ALN/aln-1* complementation line (*35Spro:ALN/aln1*; Supporting Information Fig. S4) were subjected to a 60 min drought shock, after which they were transferred back to the culture medium and grown for 7 d under standard conditions (a). Bar = 2 cm. Survival rate (b), biomass (c), chlorophyll content (d) and allantoin level (e) were evaluated for the seedlings 7 d after recovery from drought shock. FW, fresh weight. Results are the mean of three independent experiments ± standard errors of means (*$P < 0.05$, **$P < 0.01$, ***$P < 0.001$). Different letters in (e) indicate significant difference by one-way analysis of variance with Tukey's multiple comparison test ($P < 0.05$).

other purine-catabolic mutants (Fig. 4), indicating that the observed effect was specific to the *aln* mutation. Thus, we conclude that the *aln* mutation confers tolerance to osmotic stress in Arabidopsis.

To correlate purine metabolite levels with the observed stress tolerance, we measured changes in allantoin concentrations in WT and *aln* plants after stress treatments. Allantoin was consistently maintained at significantly higher levels in the two *aln* mutants than in WT, although allantoin levels increased in WT in response to drought or osmotic stress (Figs 2e & 3e). These results suggest that constitutively elevated allantoin levels in the *aln* mutants might result in enhanced tolerance to drought and osmotic stress, and that allantoin may be a critical metabolite that confers water stress protection to Arabidopsis during seedling growth.

Both *aln* mutation and exogenous allantoin administration up-regulate stress-responsive gene expression

To determine the effect of *aln* mutation on genome-wide gene expression and to correlate these effects with the stress-tolerant *aln* phenotype, we performed comparative transcript profiling with the Affymetrix ATH1 GeneChip using 2-week-old WT and *aln-1* mutant seedlings grown under normal, sterile conditions. Standard analysis of the microarray data using the Affymetrix protocols and GeneSpring software revealed that 1705 genes (988 up-regulated, 717 down-regulated) showed at least a 2.0-fold change in transcript levels between WT and the mutant. Increasing the cut-off threshold to 3.0-fold resulted in 545 genes (361 up-regulated, 184 down-regulated) displaying altered transcription in the *aln-1* mutant (Supporting Information Tables S2 & S3).

We classified the 361 up-regulated genes with at least a 3.0-fold change according to the top hierarchical level of functional categories described by the MIPS *Arabidopsis* Database (Ruepp *et al.* 2004). The significantly overrepresented genes (hypergeometric distribution: $P < 0.01$) were grouped into five functional categories (Fig. 5a); most were relevant to stress response and adaptation, such as 'Cell rescue, defence and virulence' ($P = 5.99 \times 10^{-13}$), 'Systemic interaction with the environment' ($P = 1.54 \times 10^{-7}$) and 'Interaction with the environment' ($P = 6.39 \times 10^{-6}$). Further classification at the lower levels of the MIPS functional catalogue revealed that genes assigned to functional subcategories 'Osmotic and salt stress response', 'Osmosensing and response', 'Abscisic acid response' and 'Stress response' were among the most significantly overrepresented up-regulated genes (Table 1).

We validated the microarray data by qRT-PCR to analyse expression of the five most up-regulated genes in our microarray experiments (Supporting Information Fig. S7). To gain insights into the mechanisms underlying enhanced stress tolerance in *aln* seedlings, we quantified the expression of four representative genes that are induced by ABA as well as by osmotic and drought stress (*RD29A*, *RD29B*, *RD26* and *COR15A*; Fig. 5b). As expected from the microarray data, the transcript levels of these stress-inducible genes were 2- to 16-fold higher in the *aln-1* mutant than in WT plants under normal growth conditions. However, restoring allantoin metabolism by genetic complementation totally abolished the enhanced expression of these genes exhibited by this mutant (Fig. 5b). Moreover, neither *xdh1* nor *aah* mutants showed increased levels of these transcripts relative to WT

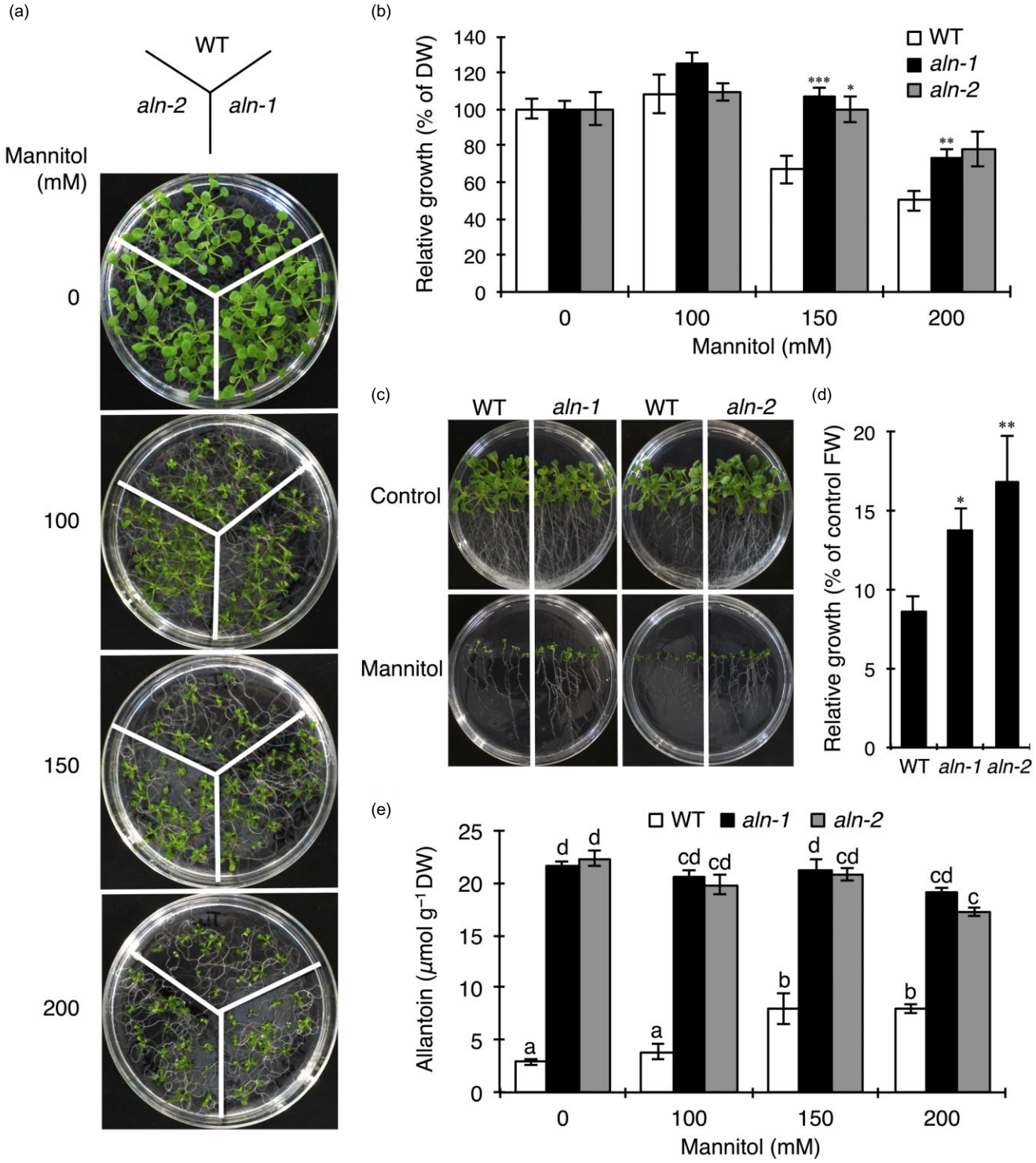

Figure 3. Tolerance of *aln-1* and *aln-2* mutants to osmotic stress imposed by mannitol. Seeds were germinated and grown for 14 d on standard medium supplemented with 100–200 mM mannitol (a, b, e) or, alternatively, 3-day-old seedlings were transferred onto standard medium containing 200 mM mannitol and grown for 14 d (c, d). Growth phenotype (a, c), relative growth (b, d) and allantoin level (e) of each genotype are shown. FW, fresh weight; DW, dry weight. The results are the mean of three independent experiments ± standard errors of means (*$P < 0.05$, **$P < 0.01$, ***$P < 0.001$). Different letters in (e) indicate significant difference by one-way analysis of variance with Tukey's multiple comparison test ($P < 0.05$).

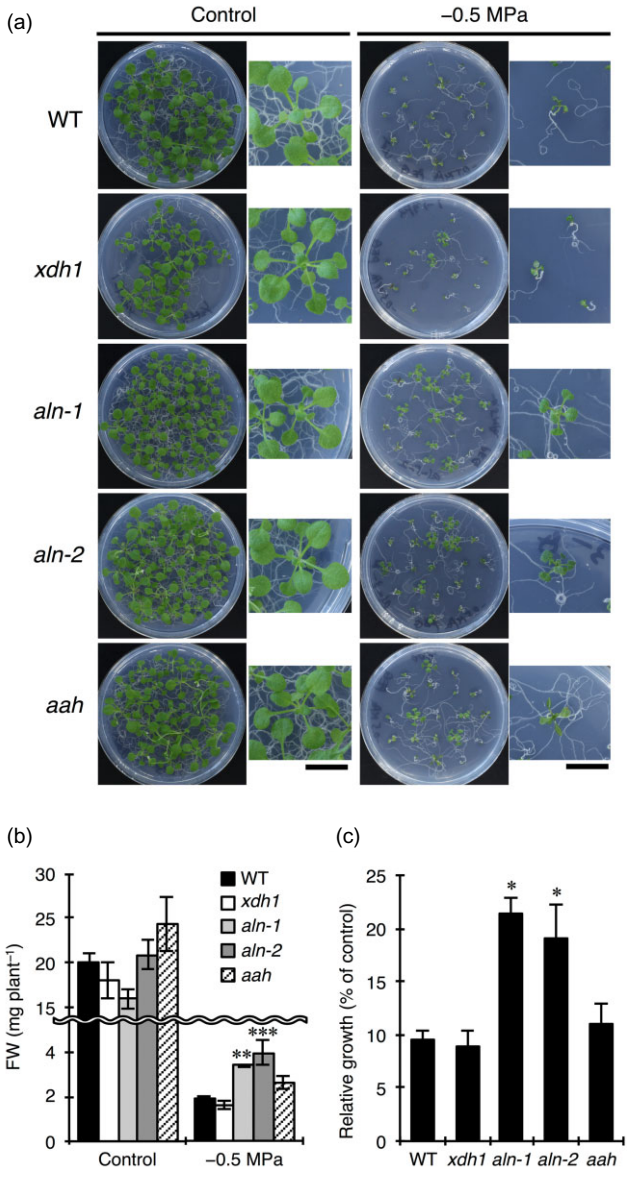

Figure 4. Tolerance of *aln-1* and *aln-2* mutants to polyethylene glycol (PEG)-mediated osmotic stress. Seeds from wild type (WT) and the four purine-catabolic mutants (*xdh1*, *aln-1*, *aln-2* and *aah*) were germinated and grown for 27 d on PEG-infused agar plates (–0.5 MPa). Growth phenotype (a), fresh weight (b) and relative growth (c) of each genotype are shown. Shown right of each picture in (a) is close-up image of representative plant growth (bar = 1 cm). FW, fresh weight. The results are the mean of three independent experiments ± standard errors of means (*$P < 0.05$, **$P < 0.01$, ***$P < 0.001$).

expression (Fig. 5c). These results suggest that the elevated allantoin levels might trigger ABA/stress-responsive gene expression without stress. To explore this possibility, the expression levels of *RD29A*, *RD29B* and *RD26* were quantified in sterile WT seedlings after treatment for 2 d with various allantoin concentrations. Exogenously supplied allantoin induced expression of these genes in a dose-dependent manner (Fig. 5d). Overall, these gene expression analyses indicate that allantoin or its accumulation evokes osmotic and drought stress responses at the gene expression level in Arabidopsis under non-stress conditions.

aln mutation increases ABA levels but does not alter the responses to ABA

To examine the possible involvement of ABA in the enhanced stress tolerance and up-regulated expression of ABA/stress-responsive genes in *aln* mutants, we measured the levels of ABA in 2-week-old sterile seedlings of WT, *aln-1*, *xdh1* and *aah* genotypes grown under normal conditions. Compared with WT seedlings, only the *aln-1* mutant showed significantly increased ABA contents among the three purine-catabolic mutants (Fig. 6a). Along with the enhanced ABA levels, the *aln-1* mutant had smaller stomatal apertures than did WT and *aah* mutants (Fig. 6b). However, stomata of detached *aln-1* leaves responded similarly as those of WT and *aah* leaves to increased concentrations of external ABA (Fig. 6c). Moreover, exogenous ABA induced ABA/stress-responsive gene expression in both *aln-1* and *aln-2* mutants at comparable levels to WT (Fig. 6d). These results suggest that the *aln* mutation mainly influences ABA metabolism but does not significantly change the sensitivity or responses to ABA.

Both *aln* mutation and exogenous allantoin administration cause activation of the critical steps in *de novo* ABA biosynthesis and hydrolysis of ABA-glucose conjugate

In Arabidopsis, two biochemical routes are the source of the stress-induced ABA accumulation: *de novo* synthesis from plastid carotenoids and deconjugation of inactive ABA-GE to regenerate ABA (Nambara & Marion-Poll 2005). We asked whether either or both of these routes were involved in the increased ABA levels in the *aln-1* mutant. Plastid-localized NCED is considered to be the rate-limiting enzyme in ABA biosynthesis in higher plants. In the *Arabidopsis* NCED family, NCED3 is responsible for drought-inducible ABA accumulation, which is essential for drought tolerance (Iuchi *et al.* 2001). The results of microarray and qRT-PCR showed that *NCED3* transcript levels increased by 3.9- and 2.4-fold, respectively, in the *aln-1* mutant compared with WT when 2-week-old seedlings were analysed (Supporting Information Table S2 & Fig. 7a). In contrast, *xdh1* and *aah* mutations had no significant effect on mRNA levels (Fig. 7a). Elevated *NCED3* expression was also evident in WT seedlings after exposure to exogenous allantoin in the growth medium for 2 d (Fig. 7b). Finally, when the *Fluc* reporter under control of the *NCED3* promoter was transiently expressed in 2-week-old plants, the dual-luciferase reporter assay revealed that the *NCED3* promoter was more active in the *aln-1* mutant than in WT (Fig. 7c).

The stress-induced increase in ABA is also mediated by the hydrolytic deconjugation of ABA-GE, which is catalysed by BG1 (also known as BGLU18), an ER-localized β-glucosidase (Lee *et al.* 2006). Under stress conditions, BG1 is

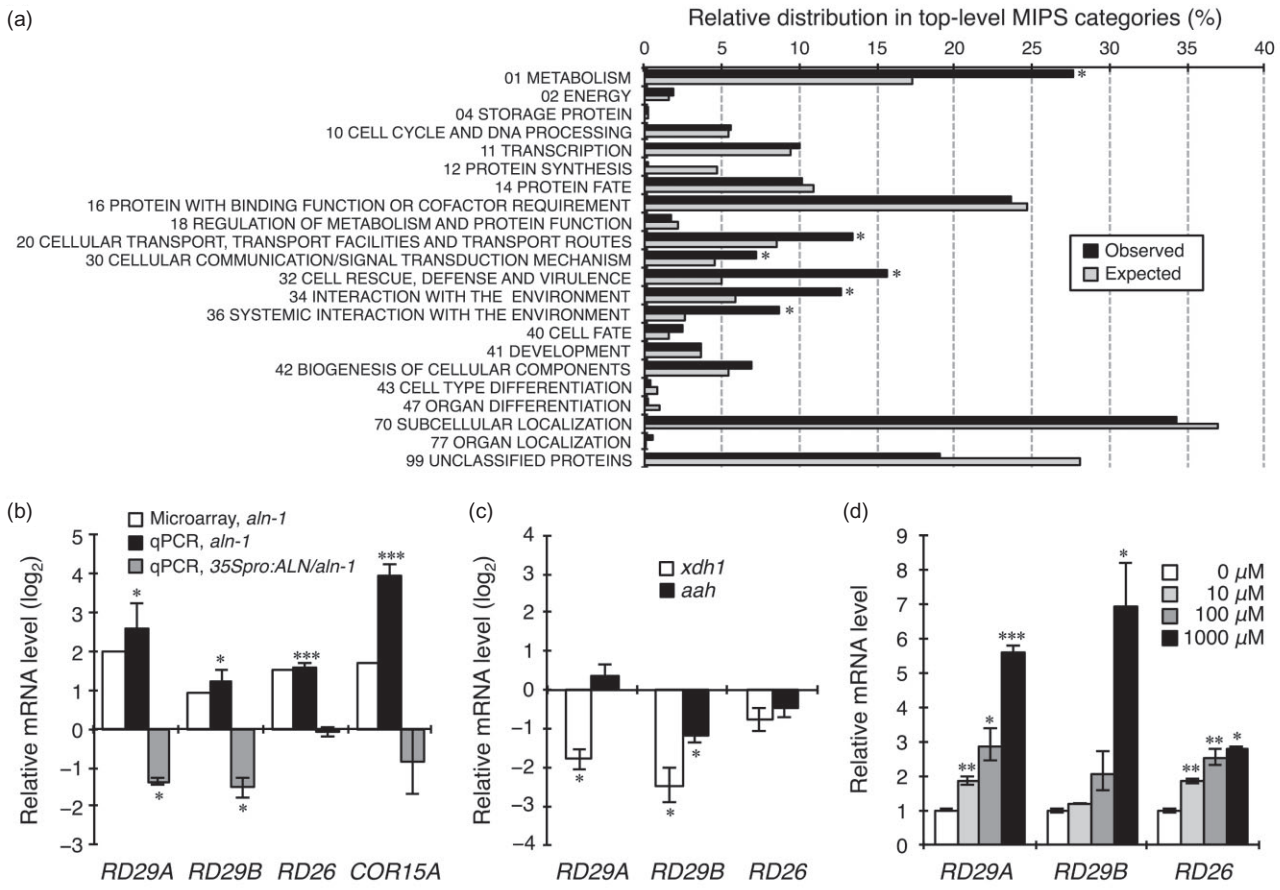

Figure 5. Allantoin accumulation enhances abscisic acid (ABA)/stress-responsive gene expression. (a) Functional classification of significantly up-regulated genes in the *aln-1* mutant. Genes up-regulated greater than threefold in the *aln-1* mutant were classified according to the top-level functional categories of Munich Information Center for Protein Sequences (MIPS; Ruepp *et al*. 2004). Black bars indicate the distribution (%) of up-regulated genes and grey bars refer to the proportion (%) of Arabidopsis genes. Asterisks indicate that the distribution of up-regulated genes differs significantly from that of Arabidopsis genes (chi-square test, $P < 0.01$). (b, c) Transcript levels of typical stress/ABA-responsive genes in the *aln-1* mutant and *ALN/aln-1* complementation line (b), and in the *xdh1* and *aah* mutants (c). Levels of the selected mRNAs were determined by microarray or qRT-PCR, using total RNA from aerial parts of 2-week-old sterile plants grown under normal conditions. Shown are $\log_2$-transformed mRNA levels relative to wild type (WT). (d) Effects of exogenous allantoin on the expression of typical stress/ABA-responsive genes in WT plants. Aseptically grown 12-day-old WT seedlings were transferred onto solid standard medium supplemented with indicated concentrations of allantoin and grown for 2 more days. *RD29A*, *RD29B* and *RD26* mRNAs were quantified by qRT-PCR using total RNA extracted from aerial parts of the plants. Results are the mean of three independent experiments ± standard errors of means (*$P < 0.05$, **$P < 0.01$, ***$P < 0.001$).

activated through polymerization of the monomer enzyme to form a high-molecular-weight (MW) complex. We compared the degree of polymerization of BG1 in WT and *aln-1* to examine the involvement of the deconjugation route in the *aln* phenotype. Native protein extracts from 2-week-old seedlings were separated by gel filtration column chromatography and the fractions were subjected to immunoblotting to detect BG1 and other proteins of known MW (Fig. 8a). Most BG1 existed predominantly as a monomer with the expected MW of 69 000 in sterile WT seedlings grown under normal conditions, and was converted into high MW forms upon drought shock. Surprisingly, normally grown *aln-1* seedlings displayed a broad distribution of BG1 in high MW fractions (more than 440 000) in addition to monomeric protein, indicating that a substantial proportion of BG1 from *aln-1* seedlings formed high-MW complexes in the absence of stress. This upward shift in MW was unique to the *aln-1* mutant and hardly observed in *xdh1* and *aah* mutants. In addition, the assembly of BG1 into high-MW forms was reproducible in non-stressed WT plants grown in the presence of allantoin (Fig. 8a), supporting the idea that allantoin may be the cause of the polymerization of BG1. Consistent with the above observations, microsomal fractions from *aln-1* seedlings possessed 2.4-fold higher ABA-GE hydrolysis activity than fractions from WT (Fig. 8b). Although compared with WT, the steady-state ABA-GE levels decreased only slightly, the ratio of ABA-GE/ABA was much lower in the *aln-1* mutant (Fig. 8c,d).

Controlling the accumulation of ABA also involves the catabolic process (Nambara & Marion-Poll 2005). We

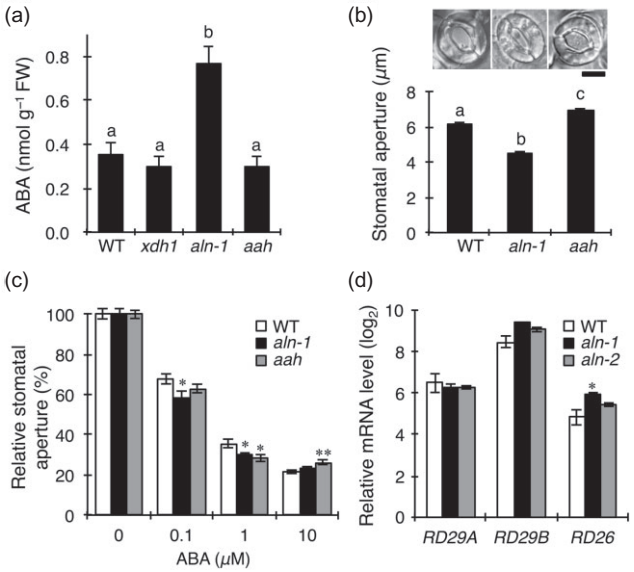

Figure 6. Effects of the *aln* mutation on abscisic acid (ABA) levels, stomatal apertures and responses to exogenous ABA. (a) ABA levels in 2-week-old wild type (WT) *aln-1*, *xdh1* and *aah* seedlings grown under standard sterile conditions. (b) The average width of stomatal apertures for leaves of WT, *aln-1* and *aah* seedlings. Pictures show microscopy images of representative stomata (bar = 10 μm). (c) Stomatal responses to exogenous ABA in WT and two *aln* mutants. Detached leaves were floated on various concentrations of ABA and the widths of the stomatal apertures were measured. Levels are shown relative to the level in the control state (no ABA). (d) Effects of exogenous ABA on typical stress/ABA-responsive genes in WT and two *aln* mutants. Aseptically grown, 2-week-old seedlings were submerged in 100 μM ABA, and after 5-h incubation, total RNA was extracted to quantify the levels of *RD29A*, *RD29B* and *RD26* mRNAs by qRT-PCR. Results are the mean of three independent experiments ± standard errors of means (*$P < 0.05$, **$P < 0.01$). Different letters in (a, b) indicate significant difference by one-way analysis of variance with Tukey's multiple comparison test ($P < 0.05$).

therefore examined the transcript levels of members of the *CYP707A* family (*CYP707A1 – CYP707A4*) encoding ABA 8′-hydroxylases, the enzymes catalysing the committed step in ABA degradation to phaseic acid. qRT-PCR revealed that *CYP707A* transcript levels were generally higher in the *aln-1* mutant, with the most up-regulated gene being *CYP707A1* (Fig. 7d), possibly reflecting the elevated ABA level in this mutant because these catabolic genes are induced by ABA (Kushiro *et al*. 2004; Saito *et al*. 2004). Taken together, these results show that elevated allantoin causes the synergistic activation of ABA metabolism, with the balance shifting towards increased ABA levels.

Exogenous allantoin increases ABA levels in WT, but not in mutants impaired in *de novo* ABA biosynthesis and hydrolysis of ABA-glucose conjugate

To gain more insights into the mechanism by which allantoin enhanced the levels of and responses to ABA, we examined the effects of exogenous allantoin on ABA accumulation and the transcript levels of ABA/stress-responsive genes (*NCED3*, *RD29A*, *RD29B* and *RD26*). We used WT and two ABA-related mutants, *aba2-1* and *bglu18*, which are impaired in the biochemical pathways leading to ABA production; specifically, *aba2-1* affects *de novo* ABA biosynthesis and *bglu18* affects BG1-catalysed deconjugation of ABA-glucose esters (Léon-Kloosterziel *et al*. 1996; Ogasawara *et al*. 2009). In WT seedlings, administration of allantoin significantly increased ABA levels by 2.5-fold (Fig. 9a), with the concomitant up-regulation of the four typical ABA/stress-responsive genes (Fig. 9b). In marked contrast to WT, the same treatment had no effect on either ABA accumulation or gene expression when applied to the two ABA-metabolic mutants. These results reveal that normal ABA production is required to elicit the *aln* phenotype in WT plants, indicating that allantoin evokes stress responses by affecting ABA levels.

DISCUSSION

In this study, our reverse-genetic and molecular approaches have provided several lines of *in planta* evidence to support

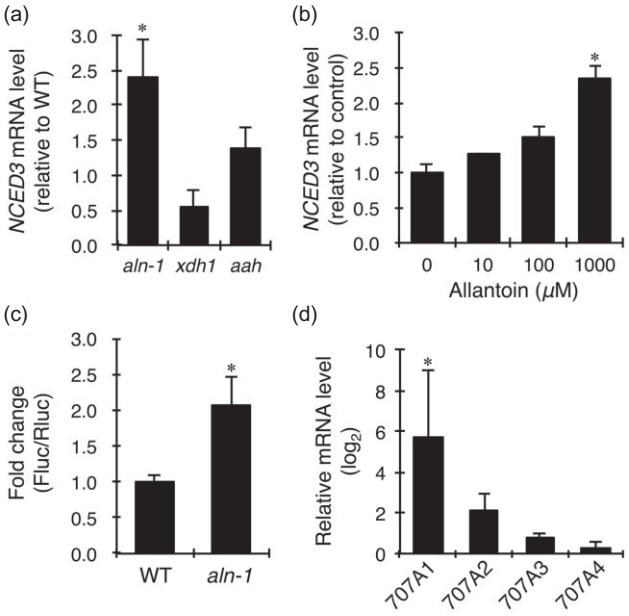

Figure 7. Allantoin accumulation induces gene expression of the rate-limiting enzymes in *de novo* abscisic acid (ABA) synthesis and degradation. (a) *NCED3* mRNA levels in 2-week-old, sterile seedlings of *aln-1*, *xdh1* and *aah* genotypes grown under normal conditions. (b) Effects of exogenous allantoin on *NCED3* expression in wild-type (WT) plants. *NCED3* transcripts were quantified as in Figure 5d. (c) *NCED3* promoter activities in WT and *aln-1* mutant. Leaves from 2-week-old seedlings were bombarded with the *NCED3* promoter/*Fluc* fusion construct. After 18-h incubation, the promoter activity was measured by dual luciferase reporter assay. (d) Relative mRNA levels of the *CYP707A* family (*CYP707A1*, *CYP707A2*, *CYP707A3* and *CYP707A4*) in 2-week-old, sterile *aln-1* seedlings grown under normal conditions. Shown are $\log_2$-transformed mRNA levels relative to WT. Results are the mean of three independent experiments ± standard errors of means (*$P < 0.05$).

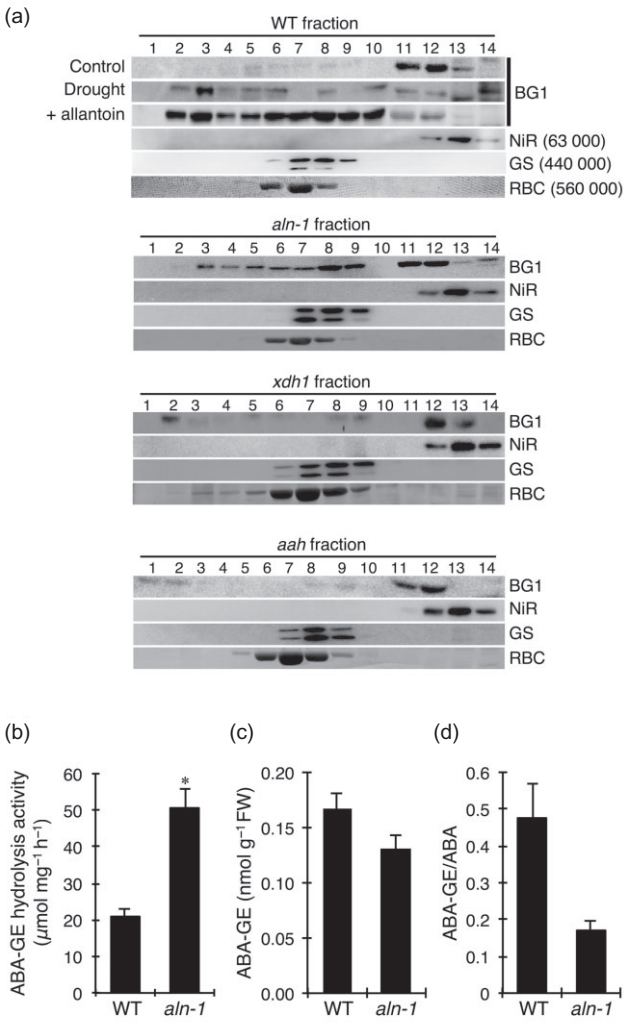

Figure 8. Allantoin accumulation activates hydrolytic deconjugation of abscisic acid-β-D-glucosyl ester (ABA-GE) to liberate ABA. (a) Molecular status of BG1 in wild type (WT), *aln-1*, *xdh1* and *aah* lines. Two-week-old sterile seedlings were used for protein extraction. Proteins were also sampled from age-matched WT seedlings after 3-h air-dry treatment (drought), or grown for 2 weeks with 100 μM allantoin (+allantoin). Protein extracts were fractionated by gel filtration column chromatography and each fraction was analysed by immunoblotting after SDS-PAGE. Labelled on the right are immunologically detected or dye-stained proteins (GS, glutamine synthetase; NiR, nitrite reductase; RBC, ribulose-1,5-bisphosphate carboxylase) with native molecular weight (MW) in parentheses, except for BG1, whose monomeric MW is ~69 000. The dual signals in GS detection correspond to plastid (upper) and cytosolic (lower) isoforms. The experiments were repeated at least twice with similar results. (b–d) ABA-GE hydrolysis activity (b), ABA-GE levels (c) and ABA-GE/ABA ratio (d) in 2-week-old, sterile WT and *aln-1* seedlings grown under normal conditions. Results are the mean of six (b) and three (c, d) independent experiments ± standard errors of means (*$P < 0.05$).

the importance of purine catabolism in stress protection of plants, with special emphasis on the critical role of the metabolic intermediate allantoin. Firstly, two independent allelic mutations in *ALN* result in enhanced seedling growth and survival under drought shock and osmotic stress conditions (Figs 2–4). Although the *aln* mutation was previously reported to have no effect on normal growth and development of Arabidopsis (Yang & Han 2004), the possible influence on stress responses and tolerance had remained unaddressed. We demonstrated that, among the three metabolic mutants deficient in specific steps in purine degradation (*xdh1*, *aln* and *aah*; Fig. 1), only *aln* mutations induced allantoin accumulation that occurred consistently with increased stress tolerance. The findings strongly suggest that allantoin has a key role in the observed stress-tolerant *aln* phenotype. Secondly, the *aln* mutant plants display genome-wide alterations in the levels of transcripts associated with stress responses and adaptation, with pronounced up-regulation of stress-inducible and ABA-regulated genes, which was not observed in either *xdh* or *aah* mutants (Fig. 5a–c & Table 1). When combined with our finding that exogenous allantoin can induce expression of typical stress/ABA-responsive genes in WT plants (Figs 5d, 7b & 9b), the results suggest the potential of allantoin in modulating the stress response at the level of gene expression. Third, *aln* mutation results in the moderate elevation of basal ABA levels (Fig. 6a), mostly due to synergistic activation of *de novo* ABA biosynthesis and deconjugation of inactive ABA conjugates (Figs 7a, c & 8). It is most plausible that the accumulated allantoin is the prime cause because these phenomena are specifically associated with *aln* but not with *xdh1* and *aah* mutations (Figs 5c, 7a & 8a), and because the exogenous allantoin reproducibly activated the two biochemical routes (Figs 7b, 8a & 9b) causing the enhanced ABA accumulation in normally grown WT seedlings (Fig. 9a). Finally, the effect of exogenous allantoin was cancelled by mutations compromised in ABA production (Fig. 9). The results, together with the observation that the *aln* mutation hardly modified the responses to exogenous ABA (Fig. 6c,d), substantiate the possible connection of purine degradation to ABA accumulation in the regulation of plant acclimatization to abiotic stress.

How allantoin contributes to stress protection has been largely unexplored until now. Allantoin has been proposed to function as an antioxidant from a few studies showing that exogenous allantoin effectively mitigated oxidative damage when administered to roots or leaf discs (Gus'kov *et al.* 2004; Brychkova *et al.* 2008). Consistent with this assumption, genetically silencing purine degradation, which decreased allantoin levels, resulted in increased H_2O_2 in transgenic Arabidopsis (Brychkova *et al.* 2008; Watanabe *et al.* 2010). However, allantoin reportedly had no direct effect *in vitro* on quenching free radicals and inhibiting lipid peroxidation (Wang *et al.* 2012). Thus, whether this particular ureide compound exerts a direct effect *in vivo* as an efficient antioxidant awaits further physiological and biochemical examination.

Apart from the above possibility, we propose another hypothesis for the role of allantoin in the acquisition of stress

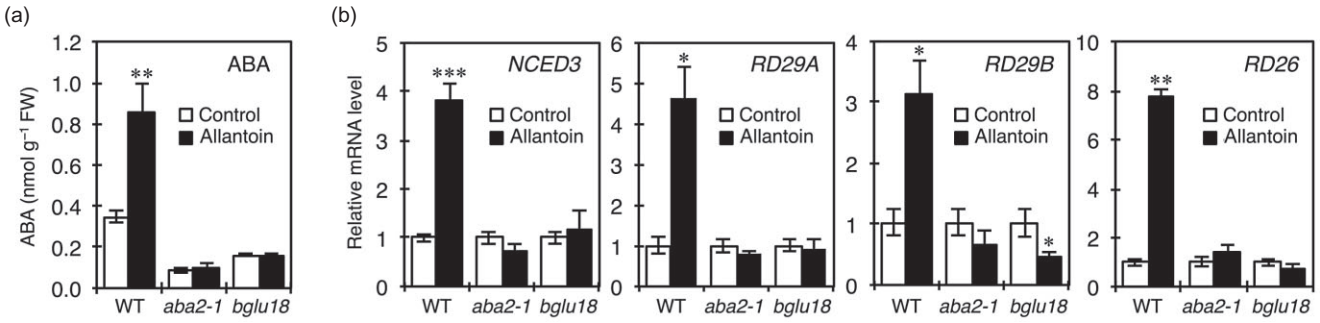

Figure 9. Effects of exogenous allantoin on abscisic acid (ABA) levels and stress/ABA-responsive gene expression in wild-type (WT) plants and two ABA-metabolic mutants, *aba2-1* and *bglu18*. (a) Endogenous ABA levels. (b) Relative mRNA levels of *NCED3*, *RD29A*, *RD29B* and *RD26*. Sterile seedlings of WT, *aba2-1* and *bglu18* were grown for 2 weeks on standard medium supplemented with 100 μM allantoin. Transcript amounts were quantified by qRT-PCR using total RNA extracted from aerial parts of the plants. FW, fresh weight. Results are the mean of three independent experiments ± standard errors of means (*$P < 0.05$, **$P < 0.01$, ***$P < 0.001$).

tolerance. The remarkable aspects of the *aln* phenotype include global changes in transcript profiles with the significant up-regulation of stress-related genes, elevated ABA levels and coordinated activation of the metabolic pathways leading to ABA accumulation (Figs 5–8), all of which are essential molecular processes for plants to respond and acclimate to water stress. It is less likely that the *aln* mutation modified ABA signalling because the responses to exogenous ABA showed little difference between WT and the *aln* mutants (Fig. 6c,d). These observations strongly indicate that the *aln* mutant is primed for stress responses probably through enhancing basal ABA levels. Allantoin is very likely responsible for the observed priming effects because most of the aforementioned phenomena were reproduced by treating WT plants with this ureide, suggesting that its possible role in stress protection is regulatory, rather than functional as proposed previously. This may explain why its antioxidant capacity was observed *in vivo* (Gus'kov *et al*. 2004; Brychkova *et al*. 2008) but not demonstrated *in vitro* (Wang *et al*. 2012). The *aln* mutants accumulated allantoin constitutively, as opposed to inducible accumulation in WT plants, but had significantly higher concentrations under both stress and non-stress conditions (Figs 2e & 3e). The stress-primed phenotype of the *aln* mutants suggests that there may be a certain threshold concentration above which allantoin could persistently evoke a key process of activating stress responses, such as accelerating ABA production (see discussion below). Consequently, we infer that, in the *aln* mutants, allantoin already exceeds such a threshold level under normal conditions while it does not reach the critical level in WT in our experimental conditions, unless supplied exogenously.

Recent studies on comparative plant physiology and metabolomics indeed imply the possibility of such a priming role for allantoin. For example, when two closely related species of *Sporobolu*s grass with highly contrasting desiccation tolerance are compared for their metabolome composition, even in the fully hydrated state, the tolerant species accumulates higher levels of osmolytes and other putative protective compounds including allantoin, suggesting that the plant is primed metabolically for drought stress (Oliver *et al*. 2011). Among rice cultivars of 15 different genotypes, there is a positive correlation between seed allantoin content and seedling survival under cold or dehydration conditions, and seed priming with allantoin significantly improves the early growth of a cultivar that accumulates little endogenous allantoin (Wang *et al*. 2012).

Our results indicate that elevated allantoin levels cause the increases in cellular ABA levels, thereby priming ABA-mediated stress responses. This raises the critical issue of how allantoin enhances ABA levels. According to the current model, stress-induced ABA production occurs mainly through two routes: *de novo* biosynthesis involving a set of plastidic and cytosolic enzymes including the rate-limiting NCED, and a simple one-step deconjugation reaction catalysed by certain β-glucosidases like BG1 allowing quick release of ABA from its inactive glucose conjugates. Under stress conditions, the former is activated by transcriptional induction of genes encoding biosynthetic enzymes while the latter requires post-translational activation of BG1 into a high-MW complex (Cheng *et al*. 2002; Barrero *et al*. 2006; Lee *et al*. 2006). We therefore examined the effects of the *aln* mutation and exogenous allantoin on *NCED3* transcription and BG1 polymerization, the key steps in the respective routes for stress-induced ABA production. We found that, without exposure to stress, these two steps were activated to increase ABA levels in the *aln* mutant and also in WT plants when administered with exogenous allantoin (Figs 7 & 8). However, the effect of allantoin on ABA production was abolished by either ABA-deficient *aba2-1* or BG1-deficient *bglu18* mutation (Fig. 9a). Of particular interest is that exogenous allantoin no longer activated *NCED3* expression in the *bglu18* mutant (Fig. 9b), even though the *de novo* biosynthetic pathway remains intact in this mutant. The observation suggests that in normally grown *aln-1* mutant and allantoin-treated WT plants, transcriptional activation of *NCED3* may be mediated, at least in part, by BG1. Constitutively activated BG1 polymers can continually liberate ABA from ABA-GE, which would allow activation of ABA biosynthesis because *NCED3* expression is strongly induced by ABA (Cheng *et al*. 2002; Barrero *et al*. 2006). This

mechanistic inference conforms to the current model for positive feedback regulation of ABA biosynthesis (Xiong *et al*. 2002).

How allantoin can promote the polymerization of BG1 is another important question to be addressed. Although BG1 monomers polymerize for activation in response to drought (Lee *et al*. 2006; and this work Fig. 8a), the molecular mechanism behind this remains largely unknown. We showed that both the endogenous allantoin accumulation in the *aln* mutant and exogenous allantoin application to WT brought about BG1 assembly into highly polymerized and enzymatically activated forms. Given that this enzyme is destined for the ER (Lee *et al*. 2006) where ureide metabolism occurs (Werner *et al*. 2008; see also Fig. 1a), it is probable that allantoin is directly involved in the mechanism of BG1 activation in this particular subcellular compartment. An intriguing observation is that the elevated level of allantoate, the immediate metabolite of allantoin (Fig. 1), failed to induce BG1 polymerization (Fig. 8a), suggesting that a certain specific interaction between BG1 and allantoin seems to lie in the basis of the possible mechanism. The nature of such possible interaction could be elucidated by *in vitro* experiments using recombinant BG1 proteins. In our experiments, the exogenous treatments with allantoin required rather high concentrations (100 to 1000 μM) to evoke ABA/stress-responsive gene expression or BG1 polymerization in WT plants. Assuming that co-localization of BG1 and allantoin may be critical for eliciting such stress responses, this may reflect the inefficiency of the exogenous treatment in increasing allantoin at physiologically effective concentrations inside the ER. The presence of ureide transporters in the plasma membrane has been demonstrated in soybean (Collier & Tegeder 2012) and it is also likely in other plants including Arabidopsis (Schmidt *et al*. 2006). However, no equivalent transport systems are known to exist for inner membranes such as ER membranes.

The *aln* mutant simultaneously enhances expression of the family of ABA 8′-hydroxylases, the key enzyme in ABA catabolism (Fig. 7d). This is an additional indication that the *aln* mutation has an impact on ABA metabolism because the ABA-dependent synergistic activation of the catabolic genes is considered to be part of the mechanism for precisely controlling ABA homeostasis (Kushiro *et al*. 2004; Saito *et al*. 2004). The results may also explain why the *aln* mutation causes increased ABA only at modest levels even though both the biosynthetic and deconjugation routes are activated in the mutant plants.

Our results suggest that allantoin degradation is a critical step of purine catabolism in plants under stress conditions. Under normal growth conditions and during the developmental progression to leaf senescence, plant purine catabolism plays a housekeeping role and allantoin is further degraded for nitrogen recycling and mobilization (Stasolla *et al*. 2003; Zrenner *et al*. 2006; Werner & Witte 2011). The use of a housekeeping metabolic intermediate in stress response and adaptation may enable prompt responses to environmental changes; stress-induced inhibition of the catabolic enzyme or down-regulation of its gene expression allows temporary accumulation of the intermediate with protective or regulatory properties. In fact, analysis of publicly available Arabidopsis microarray data (Kilian *et al*. 2007) suggests that such transcriptional regulation is likely to occur in the drought response because mRNA levels of purine-catabolic enzymes increase during normal leaf aging, but genes for these enzymes respond differentially to drought stress in an expression pattern that would result in allantoin accumulation (Supporting Information Fig. S8). Similar changes in transcriptional profiles are also reported in Arabidopsis challenged by extended dark stress (Brychkova *et al*. 2008). We hypothesized that plants could make effective use of purine catabolism for nutritional recycling or stress responses, depending on the physiological status and surrounding environmental conditions. Plants have evolved to diversify and expand their metabolism to compensate for their sessile nature, and such a dual function of a single metabolic pathway may endow plants with rapid, flexible and less costly strategies for continued growth and survival in response to constantly changing environments or changes in nutrient availability.

ACKNOWLEDGMENTS

We thank Dr. M. Nishimura (National Institute for Basic Biology) for the BG1/BGLU18 antibody, Dr. T. Nakagawa (Shimane University) for pGWB14 and pUGW35 and Dr. T. Konishi (Akita Prefectural University) for discussion of microarray analysis. Supported in part by Grant-in-Aid for Scientific Research on Innovative Areas (Nos. 23119514 and 25119717 to A.S.) from the Ministry of Education, Culture, Sports, Science and Technology of Japan on 'Integrated Analysis of Strategies for Plant Survival and Growth in Response to Global Environmental Changes', a Grant-in-Aid for Scientific Research (No. 22570043 to A.S.) from the Japan Society for the Promotion of Science (JSPS) and the Joint Research Program of Arid Land Research Center, Tottori University (to A.S.). S.W. was a recipient of a Grant-in-Aid for JSPS Fellows (DC2, no. 23-7275).

REFERENCES

Alamillo J.M., Dí Az-Leal J.L., Sánchez-Moran M.A.V. & Pineda M. (2010) Molecular analysis of ureide accumulation under drought stress in *Phaseolus vulgaris* L. *Plant, Cell & Environment* **33,** 1828–1837.

Barrero J., Rodríguez P.L., Quesada V., Piqueras P., Ponce M.R. & Micol J.L. (2006) Both abscisic acid (ABA)-dependent and ABA-independent pathways govern the induction of *NCED3*, *AAO3* and *ABA1* in response to salt stress. *Plant, Cell & Environment* **29,** 2000–2008.

Brychkova G., Alikulov Z., Fluhr R. & Sagi M. (2008) A critical role for ureides in dark and senescence-induced purine remobilization is unmasked in the *Atxdh1* Arabidopsis mutant. *The Plant Journal* **54,** 496–509.

Cheng W.H., Endo A., Zhou L., Penney J., Chen H.C., Arroyo A., . . . Sheen J. (2002) A unique short-chain dehydrogenase/reductase in Arabidopsis glucose signaling and abscisic acid biosynthesis and functions. *The Plant Cell* **14,** 2723–2743.

Clough S.J. & Bent A.F. (1998) Floral dip: a simplified method for *Agrobacterium*-mediated transformation of *Arabidopsis thaliana*. *The Plant Journal* **16,** 735–743.

Collier R. & Tegeder M. (2012) Soybean ureide transporters play a critical role in nodule development, function and nitrogen export. *The Plant Journal* **72,** 355–367.

Dietz K.J., Sauter A., Wichert K., Messdaghi D. & Hartung W. (2000) Extracellular β-glucosidase activity in barley involved in the hydrolysis of ABA glucose conjugate in leaves. *Journal of Experimental Botany* **51,** 937–944.

Gus'kov E.P., Prokof'ev V.N., Kletskii M.E., Kornienko I.V., Gapurenko O.A., Olekhnovich L.P., . . . Zhdanov Y.A. (2004) Allantoin as a vitamin. *Doklady Biochemistry and Biophysics* **398,** 823–827.

Hesberg C., Hansch R., Mendel R.R. & Bittner F. (2004) Tandem orientation of duplicated xanthine dehydrogenase genes from *Arabidopsis thaliana*: differential gene expression and enzyme activities. *Journal of Biological Chemistry* **279,** 13547–13554.

Iuchi S., Kobayashi M., Taji T., Naramoto M., Seki M., Kato T., . . . Shinozaki K. (2001) Regulation of drought tolerance by gene manipulation of 9-*cis*-epoxycarotenoid dioxygenase, a key enzyme in abscisic acid biosynthesis in *Arabidopsis*. *The Plant Journal* **27,** 325–333.

Kanani H., Dutta B. & Klapa M.I. (2010) Individual vs. combinatorial effect of elevated CO_2 conditions and salinity stress on *Arabidopsis thaliana* liquid cultures: comparing the early molecular response using time-series transcriptomic and metabolomic analyses. *BMC Systems Biology* **4,** 177.

Kilian J., Whitehead D., Horak J., Wanke D., Weinl S., Batistic O., . . . Harter K. (2007) The AtGenExpress global stress expression data set: protocols, evaluation and model data analysis of UV-B light, drought and cold stress responses. *The Plant Journal* **50,** 347–363.

Kushiro T., Okamoto M., Nakabayashi K., Yamagishi K., Kitamura S., Asami T., . . . Nambara E. (2004) The *Arabidopsis* cytochrome P450 CYP707A encodes ABA 8′-hydroxylases: key enzymes in ABA catabolism. *The EMBO Journal* **23,** 1647–1656.

Lee K.H., Piao H.L., Kim H.Y., Choi S.M., Jiang F., Hartung W., . . . Hwang I. (2006) Activation of glucosidase via stress-induced polymerization rapidly increases active pools of abscisic acid. *Cell* **126,** 1109–1120.

Léon-Kloosterziel K.M., Gil M.A., Ruijs G.J., Jacobsen S.E., Olszewski N.E., Schwartz S.H., . . . Koornneef M. (1996) Isolation and characterization of abscisic acid-deficient *Arabidopsis* mutants at two new loci. *The Plant Journal* **10,** 655–661.

Livak K.J. & Schmittgen T.D. (2001) Analysis of relative gene expression data using real-time quantitative PCR and the $2^{-\Delta\Delta Ct}$ Method. *Methods* **25,** 402–408.

Montalbini P. (1991) Effect of rust infection on levels of uricase, allantoinase and ureides in susceptible and hypersensitive bean leaves. *Physiological and Molecular Plant Pathology* **39,** 173–188.

Montalbini P. (1995) Effect of rust infection on purine catabolism enzyme levels in wheat leaves. *Physiological and Molecular Plant Pathology* **46,** 275–292.

Nakagawa A., Sakamoto S., Takahashi T., Morikawa H. & Sakamoto A. (2007a) The RNAi-mediated silencing of xanthine dehydrogenase impairs growth and fertility and accelerates leaf senescence in transgenic Arabidopsis plants. *Plant and Cell Physiology* **48,** 1484–1495.

Nakagawa T., Kurose T., Hino T., Tanaka K., Kawamukai M., Niwa Y., . . . Kimura T. (2007b) Development of series of gateway binary vectors, pGWBs, for realizing efficient construction of fusion genes for plant transformation. *Journal of Bioscience and Bioengineering* **104,** 34–41.

Nambara E. & Marion-Poll A. (2005) Abscisic acid biosynthesis and catabolism. *Annual Review of Plant Biology* **56,** 165–185.

Nikiforova V.J., Kopka J., Tolstikov V., Fiehn O., Hopkins L., Hawkesford M.J., . . . Hoefgen R. (2005) Systems rebalancing of metabolism in response to sulfur deprivation, as revealed by metabolome analysis of Arabidopsis plants. *Plant Physiology* **138,** 304–318.

Ogasawara K., Yamada K., Christeller J.T., Kondo M., Hatsugai N., Hara-Nishimura I. & Nishimura M. (2009) Constitutive and inducible ER bodies of *Arabidopsis thaliana* accumulate distinct β-glucosidases. *Plant and Cell Physiology* **50,** 480–488.

Oliver M.J., Guo L., Alexander D.C., Ryals J.A., Wone B.W. & Cushman J.C. (2011) A sister group contrast using untargeted global metabolomic analysis delineates the biochemical regulation underlying desiccation tolerance in *Sporobolus stapfianus*. *The Plant Cell* **23,** 1231–1248.

Pei Z.M., Kuchitsu K., Ward J.M., Schwarz M. & Schroeder J.I. (1997) Differential abscisic acid regulation of guard cell slow anion channels in Arabidopsis wild-type and *abi1* and *abi2* mutants. *The Plant Cell* **9,** 409–423.

Rose M.T., Rose T.J., Pariasca-Tanaka J., Yoshihashi T., Neuweger H., Goesmann A., . . . Wissuwa M. (2012) Root metabolic response of rice (*Oryza sativa* L.) genotypes with contrasting tolerance to zinc deficiency and bicarbonate excess. *Planta* **236,** 959–973.

Ruepp A., Zollner A., Maier D., Albermann K., Hani J., Mokrejs M., . . . Mewes H.W. (2004) The FunCat, a functional annotation scheme for systematic classification of proteins from whole genomes. *Nucleic Acids Research* **32,** 5539–5545.

Sagi M., Omarov R.T. & Lips S.H. (1998) The Mo-hydroxylases xanthine dehydrogenase and aldehyde oxidase in ryegrass as affected by nitrogen and salinity. *Plant Science* **135,** 125–135.

Saito S., Hirai N., Matsumoto C., Ohigashi H., Ohta D., Sakata K. & Mizutani M. (2004) Arabidopsis *CYP707A*s encode (+)-abscisic acid 8′-hydroxylase, a key enzyme in the oxidative catabolism of abscisic acid. *Plant Physiology* **134,** 1439–1449.

Sakamoto A., Takeba G. & Tanaka K. (1990) Synthesis de novo of glutamine synthetase in the embryonic axis, closely related to the germination of lettuce seeds. *Plant and Cell Physiology* **31,** 677–682.

Schmidt A., Baumann N., Schwarzkopf A., Frommer W.B. & Desimone M. (2006) Comparative studies on Ureide Permeases in *Arabidopsis thaliana* and analysis of two alternative splice variants of *AtUPS5*. *Planta* **224,** 1329–1340.

Schubert K.R. (1986) Products of biological nitrogen fixation in higher plants: synthesis, transport, and metabolism. *Annual Review of Plant Physiology* **37,** 539–574.

Shigeto J., Yoshihara S., Adam S.E.H., Sueyoshi K., Sakamoto A., Morikawa H. & Takahashi M. (2006) Genetic engineering of nitrite reductase gene improves uptake and assimilation of nitrogen dioxide by *Rhaphiolepis umbellata* (Thunb.) Makino. *Plant Biotechnology* **23,** 111–116.

Smith P.M.C. & Atkins C.A. (2002) Purine biosynthesis. Big in cell division, even bigger in nitrogen assimilation. *Plant Physiology* **128,** 793–802.

Stasolla C., Katahira R., Thorpe T.A. & Ashihara H. (2003) Purine and pyrimidine nucleotide metabolism in higher plants. *Journal of Plant Physiology* **160,** 1271–1295.

Todd C.D. & Polacco J.C. (2006) *AtAAH* encodes a protein with allantoate amidohydrolase activity from *Arabidopsis thaliana*. *Planta* **223,** 1108–1113.

Verslues P.E., Agarwal M., Katiyar-Agarwal S., Zhu J. & Zhu J.K. (2006) Methods and concepts in quantifying resistance to drought, salt and freezing, abiotic stresses that affect plant water status. *The Plant Journal* **45,** 523–539.

Vogels G.D. & Van der Drift C. (1976) Degradation of purines and pyrimidines by microorganisms. *Bacteriological Reviews* **40,** 403–468.

Wang P., Kong C.H., Sun B. & Xu X.H. (2012) Distribution and function of allantoin (5-ureidohydantoin) in rice grains. *Journal of Agricultural and Food Chemistry* **60,** 2793–2798.

Watanabe S., Nakagawa A., Izumi S., Shimada H. & Sakamoto A. (2010) RNA interference-mediated suppression of xanthine dehydrogenase reveals the role of purine metabolism in drought tolerance in Arabidopsis. *FEBS Letters* **584,** 1181–1186.

Werner A.K. & Witte C. (2011) The biochemistry of nitrogen mobilization: purine ring catabolism. *Trends in Plant Science* **16,** 381–387.

Werner A.K., Sparkes I.A., Romeis T. & Witte C.-P. (2008) Identification, biochemical characterization, and subcellular localization of allantoate amidohydrolases from Arabidopsis and soybean. *Plant Physiology* **146,** 418–430.

Xiong L., Lee H., Ishitani M. & Zhu J.K. (2002) Regulation of osmotic stress-responsive gene expression by the *LOS6*/*ABA1* locus in *Arabidopsis*. *Journal of Biological Chemistry* **277,** 8588– 8596.

Yan J., Tsuichihara N., Etoh T. & Iwai S. (2007) Reactive oxygen species and nitric oxide are involved in ABA inhibition of stomatal opening. *Plant, Cell & Environment* **30,** 1320–1325.

Yang J. & Han K.-H. (2004) Functional characterization of allantoinase genes from Arabidopsis and a nonureide-type legume black locust. *Plant Physiology* **134,** 1039–1049.

Yesbergenova Z., Yang G., Oron E., Soffer D., Fluhr R. & Sagi M. (2005) The plant Mo-hydroxylases aldehyde oxidase and xanthine dehydrogenase have distinct reactive oxygen species signatures and are induced by drought and abscisic acid. *The Plant Journal* **42,** 862–876.

Yobi A., Wone B.W., Xu W., Alexander D.C., Guo L., Ryals J.A., . . . Cushman J.C. (2013) Metabolomic profiling in *Selaginella lepidophylla* at various hydration states provides new insights into the mechanistic basis of desiccation tolerance. *Molecular Plant* **6,** 369–385.

Zrenner R., Stitt M., Sonnewald U. & Boldt R. (2006) Pyrimidine and purine biosynthesis and degradation in plants. *Annual Review of Plant Biology* **57,** 805–836.

Received 26 April 2013; accepted for publication 4 October 2013

SUPPORTING INFORMATION

Additional Supporting Information may be found in the online version of this article at the publisher's web-site:

Figure S1. Characterization of two allelic *aln* mutants.
Figure S2. Characterization of an *xdh1* mutant.
Figure S3. Characterization of an *aah* mutant.
Figure S4. Genetic complementation of *aln-1* mutation by *ALN* overexpression.
Figure S5. Effects of osmotic stress imposed by mannitol on seed germination of WT and *aln* mutants.
Figure S6. Effects of osmotic stress imposed by PEG on seed germination of WT and the four purine-catabolic mutants.
Figure S7. Confirmation of the microarray expression data for the five most strongly up-regulated genes in the *aln-1* mutant by qRT-PCR.
Figure S8. Coordinated and differential expression of purine catabolic enzymes in Arabidopsis.
Table S1. Nucleotide sequences of primers used in this study.
Table S2. List of the up-regulated genes in the *aln-1* mutant.
Table S3. List of the down-regulated genes in the *aln-1* mutant.